



1 **Development of a hydrological ensemble prediction system and a**
2 **visualization approach for improved interpretation during typhoon**
3 **events**

4 Sheng-Chi Yang¹, Tsun-Hua Yang¹, Ya-Chi Chang^{1,*}, Cheng-Hsin Chen¹, Mei-Ying
5 Lin¹, Jui-Yi Ho¹ and Kwan-Tun Lee^{1,2}

6 ¹Taiwan Typhoon and Flood Research Institute (TTFRI), National Applied Research Laboratories
7 (NARLabs), Taipei, Taiwan

8 ²Department of River and Harbor Engineering, National Taiwan Ocean University, Keelung, Taiwan

9 *Correspondence to: 11 F, No. 97, Sec. 1, Roosevelt Rd., Zhongzheng Dist., Taipei City 10093, Taiwan
10 (R.O.C.)

11 E-mail: rachel.ev91@gmail.com

12

13 **ABSTRACT**

14 Typhoons are accompanied by heavy rainfall and cause loss of life and property.

15 Hydrological ensemble prediction systems can provide decision makers with

16 hydrological information, such as peak stage and peak time, with some lead time. This

17 information assists decision makers in taking the necessary measures to prevent and

18 mitigate disasters. This study proposes a hydrological ensemble prediction system that

19 includes numerical weather models that perform rainfall forecasts and hydrologic

20 models that produce assessments of surface runoff and the associated flooding.

21 However, the spatiotemporal uncertainty associated with the numerical models and the

22 difficulty in interpreting the model results hinder effective decision making during

23 emergency response situations. Thus, this study also presents an extension of the ‘Peak-



24 Box' visualization methodology that assists in interpreting the forecast results for
25 operational purposes. A small watershed with area of 100 km² and four typhoons that
26 occurred from 2012 to 2015 were selected to evaluate the performance of these tools.
27 The results showed that the modified visualization approach improved the intelligibility
28 of forecasts of the peak stages and peak times compared to that of approaches
29 previously described in the literature. The new approach includes all available forecasts
30 to increase the sample size. The capture rate is greater than 50%, which is considered
31 practical for decision makers. The proposed system and the modified visualization
32 approach have demonstrated their potential for both decreasing the uncertainty of
33 numerical rainfall forecasts and improving the performance of flood forecasts.

34

35 **KEY WORDS** Hydrological ensemble prediction system; peak flow; decision support;
36 visualization.

37



38

1. INTRODUCTION

39

Numerical weather prediction (NWP) models generate different precipitation

40

forecasts for specified locations and times due to the incompleteness of the input

41

observations, the approximate nature of the forecast models and their parameterizations,

42

and the random errors that result from perturbing the initial atmospheric conditions

43

(Palmer, 2001; Hostache et al., 2011). Ensemble prediction systems (EPSs), which

44

consist of an adequate number of equiprobable NWP models, have been established to

45

provide probabilistic precipitation forecasts instead of a single deterministic forecast

46

(Cloke and Pappenberger, 2009). An EPS provides predictions with greater skill than

47

those obtained from individual runs of NWP models or deterministic model runs,

48

especially for longer lead times (Demeritt et al., 2007; Cuo et al., 2011).

49

A hydrological ensemble prediction system (HEPS) is an integrated system that

50

couples an EPS with catchment-scale hydrological models to provide flood forecasts

51

with sufficient lead time. The importance of such systems in disaster mitigation, water

52

resource management, and hydropower dam and lake operation is growing

53

(Pappenberger et al., 2005; Cloke and Pappenberger, 2009; Zappa et al., 2010, 2013;

54

Yang and Yang, 2014). However, uncertainties stemming from factors including

55

boundary conditions, initial conditions, and model parameter values affect the forecast

56

accuracy of these systems. The precipitation forecasts of NWP models dominate the



57 overall uncertainty of these systems (Zappa et al., 2011; Rossa et al., 2011). It is
58 necessary to develop guidelines and tools for communicating the uncertainties
59 associated with complex HEPSs (e.g., Jaun et al., 2008; Thielen et al., 2009; Bartholmes
60 et al., 2009; Todini, 2009; Bruen et al., 2010; Renard et al., 2010; Thirel et al., 2010;
61 Zappa et al., 2010, 2013; Frick and Hegg, 2011; Pappenberger et al., 2011a, 2011b;
62 Fundel and Zappa, 2011; Pappenberger et al., 2013).

63 Effective communication of ensemble forecasts means that clear expression of the
64 uncertainties associated with HEPS is important so that end-users can easily respond to
65 the information provided during operations (Demeritt et al., 2010; Ramos et al., 2010;
66 Pappenberger et al., 2013; Zappa et al., 2013; Pagano et al., 2014). Pagano et al. (2014)
67 noted that defining effective methods for the communication of ensemble forecasts is a
68 challenge for future operational river forecasting and represents a future research
69 opportunity. Pappenberger et al. (2013) argued that the uncertainty information
70 provided by HEPSs sometimes results in resistance on the part of the public if experts
71 or nonexperts cannot easily understand the information provided. At present, HEPSs
72 still rely on conventional visualization techniques, such as ‘spaghetti diagrams’ or box
73 plots, to display the distributions of forecast results. Pappenberger et al. (2013) focused
74 on expert users of HEPSs and the communication among these experts and identified
75 key information for the public, such as discharge, lead time, warning levels, return



76 periods, worst/best scenario, etc. Zappa et al. (2013) proposed the ‘Peak-Box’
77 visualization approach to support the interpretation and verification of HEPS results.
78 This approach has been used to obtain quantitative and qualitative insights, such as the
79 timing, water level, and discharge associated with peak flow. This information is crucial
80 for end-users and decision makers. Zappa et al. (2013) applied an operational HEPS,
81 namely, the IFKIS-HYDRO hydrological nowcasting system, to five different basins in
82 Switzerland to evaluate the performance of the ‘Peak-Box’ methodology. The sizes of
83 the basins ranged from 186 km² to 1696 km². The study found that, of 485 operational
84 forecasts performed from June 2007 through November 2008, 30% to 55% of the
85 observed peaks fell outside the ‘Peak-Box’.



86 Typhoons are common natural events that cause severe damage in countries at the
87 edge of the northwestern Pacific Ocean, such as Japan, the Philippines, and Taiwan. For
88 example, based on records covering 1958 to 2010, an average of 3.4 typhoons affect
89 Taiwan annually, and these events cause an annual average loss of more than 500
90 million U.S. dollars (Li et al., 2004). Typhoon-related flood events cause these losses.
91 If they provide early warnings with sufficient lead time, flood forecasts from a HEPS
92 can help authorities prepare disaster prevention and mitigation measures. A customized
93 visualization method for typhoons is also necessary to make the ensemble flood
94 forecasts generated by HEPS meaningful for emergency responders. Therefore, this



95 study presents a HEPS that can provide ensemble flood forecasts during typhoon events
96 and proposes a customized visualization approach especially for typhoons to simplify
97 the forecast information. This approach is an extension of the one presented by Zappa
98 et al. (2013); it has been modified to increase the percentage of observed peaks that fall
99 within the predicted range during typhoon events. The remainder of this paper is
100 organized as follows. Section 2 includes the details of the proposed HEPS. Section 3
101 briefly describes the study area and typhoon events used in the study. Section 4
102 compares the original ‘Peak-Box’ approach with the proposed extended version. Finally,
103 Sect. 5 and 6 present the results, discussion, and conclusions.

104 2. SETUP OF THE HYDROLOGICAL ENSEMBLE PREDICTION 105 SYSTEM

106 This study proposes a HEPS that integrates various models. These models include
107 NWP models that provide ensemble precipitation forecasts, a rainfall-runoff model that
108 generates upstream boundary conditions, a storm surge model that generates
109 downstream boundary conditions, and a flood routing model that simulates river flows.
110 The data processing is shown in Figure 1. The HEPS produces ensemble flood forecasts
111 with a 72-hour lead time four times a day. The models used in the HEPS are described
112 in the following subsections.



113 2.1 Ensemble precipitation forecasts

114 The Taiwan Cooperative Precipitation Ensemble Forecast Experiment (TAPEX)

115 began in 2010. It is a collective effort among academic institutes and government

116 agencies, such as the National Taiwan University, the National Central University, the

117 National Taiwan Normal University, the Chinese Culture University, the Central

118 Weather Bureau (CWB), the National Center for High-Performance Computing, the

119 Taiwan Typhoon and Flood Research Institute (TTFRI), and the National Science and

120 Technology Center for Disaster Reduction. TAPEX is the first attempt to design a high-

121 resolution (5-km) numerical ensemble model in Taiwan. This effort applies various

122 NWP models, such as the Weather Research and Forecasting Model (WRF), the Fifth-

123 Generation Penn State/NCAR Mesoscale Model (MM5), the Cloud-Resolving Storm

124 Simulator (CReSS), and the Hurricane Weather Research and Forecasting Model

125 (HWRF). It also considers different setups in terms of the model initial conditions, data

126 assimilation processes and model physics. TAPEX generates four runs a day and

127 provides ensemble predictions of the wind and pressure fields and quantitative

128 estimates of precipitation with a lead time of 72 hours. Further information can be found

129 in Hsiao et al. (2013). A typhoon's average impact duration is 73.68 hours (Huang et

130 al., 2012) and the average lag between observed peak precipitation and flooding in

131 Taiwan is between 2 and 10 hours (Jang et al., 2012). This study focuses on a one-way



132 coupling in which TAPEX provides rainfall forecast to the rainfall-runoff model;
133 feedbacks from the rainfall-runoff model to TAPEX are not considered.

134 *2.2 Rainfall-runoff model*

135 The HEPS uses the surface runoff forecast generated by a kinematic-wave-based
136 geomorphologic instantaneous unit hydrograph model (the KW-GIUH model) as its
137 upstream boundary condition. The KW-GIUH model, which was developed by Lee and
138 Yen (1997), can reflect the effects of watershed geomorphology, land cover conditions,
139 soil characteristics and rainfall intensity on runoff. It has been successfully applied to
140 many Taiwanese catchments (Lee et al., 2001; 2006).

141 *2.3 Storm surge model*

142 Storm surges are abnormal increases in water levels above those expected from
143 astronomical tides. They are generated by strong winds and atmospheric pressure
144 changes and affect water levels downstream (near estuaries) during typhoons. The
145 HEPS uses the storm surge and tide forecasts generated by the Princeton Ocean Model
146 (POM) and the TOPEX-POSEIDON global tidal model (TPXO6.2) as downstream
147 boundary conditions. The POM model, which was developed by Blumberg and Mellor
148 (1987), is a three-dimensional, nonlinear, primitive equation finite difference ocean
149 model. It has been applied to simulate a wide range of ocean problems, including
150 coastal storm surge in Taiwan (Ou et al., 2008; Chiou, 2010). In this study, the TAPEX



151 model provides ensemble pressure field and wind field forecasts to POM and the
152 TPXO6.2 model and obtains tidal level predictions. As with TAPEX, it generates four
153 runs a day, and each run has a 72-hour lead time.

154 *2.4 Flood routing model*

155 The Numerical Model Simulating Water Flow and Contaminant and Sediment
156 Transport in WAterSHed Systems of 1D Stream/River Networks, 2D Overland
157 Regimes, and 3D Subsurface Media (WASH123D) was developed by Yeh et al. (1998)
158 to simulate one-dimensional channel networks, two-dimensional overland flow, and
159 three-dimensional variably saturated subsurface flow. It has been applied successfully
160 in Taiwan and around the world, and it was chosen by the US Army Corps of Engineers
161 as the core computational code used in modeling the Lower East Coast (LEC) Wetland
162 Watershed (e.g., Yeh et al., 2006; Yeh and Shih., 2011; Shih et al., 2012; Hsiao et al.,
163 2013). The HEPS uses the one-dimensional channel model of WASH123D as its flood
164 routing model to simulate water stages in rivers.

165 3. STUDY AREA AND TYPHOON EVENTS

166 *3.1 Study area*

167 This study selected the Yilan River in northeastern Taiwan as the study area
168 (Figure 2). The river flows through the city of Yilan and has a main stream length of
169 approximately 24.4 km and a watershed area of 149.06 km². It has four main tributaries,



170 which are the Wushi River, the Dahu River, the Dajiao River and the Xiaojiao River.

171 The Water Resource Agency (WRA) and TTFRI have selected this river as one of two

172 watersheds where long-term monitoring experiments are being carried out (the other is

173 the Dianbao Creek basin in southwestern Taiwan). The purpose of the experimental

174 watersheds is to generate long-term and high-density hydrological monitoring data that

175 can be used for scientific studies, including the development of hydrological and

176 hydraulic models and the study of environmental changes. In total, 11 rainfall gauging

177 stations, 16 water-stage gauging stations, five river-velocity gauging stations, and 36

178 inundation-depth gauging stations have been installed in the Yilan River Basin. Figure

179 2 shows the locations of the water-stage and rainfall gauging stations that collected the

180 data that we used in this study. The monitoring data have been carefully collected and

181 processed. For full information and to download the available data, please refer to the

182 official website (<http://wraew.ttfri.narl.org.tw/index.php>).

183 TAPEX provides 72-hour rainfall forecasts for five rainfall gauges in the upstream

184 portion of the Yilan River Basin. The KW-GIUH model calculates the surface runoff

185 and estimates river flow at the Hsincheng and Yuanshan Bridges. This study uses the

186 POM and TPXO6.2 models to forecast the tides at Suao and to estimate the water stages

187 at the Kemalan Bridge. WASH123D then generates ensemble flow forecasts using

188 flows at the bridges mentioned above as the upstream boundary condition and the water



189 stage at the Kemalan Bridge as the downstream boundary condition. The detailed
190 locations of these places are shown in Figure 2.

191 3.2 Typhoon events

192 Figure 3 shows the tracks of the different typhoons that have affected Taiwan,
193 according to historical records (Huang et al., 2012). Of the ten categories, Type-2 and
194 Type-3 typhoons account for approximately 28% of all typhoons and bring heavy
195 rainfall to the Yilan River Basin. For instance, a rainfall of 158 mm in 4 hours was
196 observed at rainfall gauging station C1U610 (shown in Figure 2) during Typhoon
197 Soulik. Table 1 shows all of the typhoons that invaded Taiwan from 2012 through 2015.
198 Five of these events are Type-2 and Type-3 typhoons, which have the biggest impact
199 on the Yilan River Basin. Therefore, this study selected the typhoons Saola (2012),
200 Soulik (2013), Soudelor (2015), and Dujuan (2015) to calibrate the HEPS and test its
201 performance. Typhoon Matmo, a Type-3 typhoon that occurred in 2014, was not
202 included due to its weak intensity. This study used historical observations of rainfall,
203 river stage, and tide to validate the parameters in the proposed HEPS.

204 4. A VISUALIZATION APPROACH FOR SUPPORTING THE 205 INTERPRETATION OF OPERATIONAL ENSEMBLE PEAK-



206 FLOW FORECASTS DURING TYPHOON EVENTS

207 This study modified the ‘Peak-Box’ approach originally proposed by Zappa et al.
 208 (2013) to provide better communication of HEPS forecasts during typhoon events.
 209 Figure 4 compares the two approaches, and the modifications are described in detail
 210 below. The purpose of the modifications is to develop a visualization approach that
 211 simplifies the ensemble flow forecast information for use in formulating emergency
 212 responses during typhoon events.

213 a. **Remove the horizontal and the vertical lines.** The horizontal and vertical lines
 214 that indicate the medians of ensemble forecasts in the original ‘Peak-Box’ approach
 215 are removed to prevent some information from being misused. Although
 216 uncertainties exist in the HEPS, Pappenberger et al. (2013) noted a considerable
 217 desire on the part of end-users to reduce probabilistic forecasts to deterministic
 218 actions. The two lines may lead end-users to believe that the information provided
 219 represents a single deterministic forecast, rather than a probabilistic one.

220 b. **Remove the outer rectangle.** In the original ‘Peak-Box’ approach, two rectangles
 221 are displayed. The outer rectangle is the ‘Peak-Box,’ which highlights all
 222 possibilities from the ensemble forecast, and the inner rectangle is the ‘IQR-Box’
 223 that emphasizes the 25th and 75th percentiles of the peak times and peak discharges
 224 of the ensemble forecast. Zappa et al. (2013) argued that the outer rectangle



225 provides the forecaster with additional information. However, this argument does
 226 not hold during typhoons, when the availability of too much data may obscure
 227 critical information. Therefore, only one rectangle is shown in the study. This
 228 rectangle indicates where the observed peak stage is likely to occur.

229 c. **Use the mean and the standard deviation to define the rectangle.** This study
 230 defines an ‘SD-Box’ that uses the mean (μ) and the standard deviation (σ), instead
 231 of the first and third quartiles, to define the enveloping rectangle. As shown in the
 232 right panel of Figure 4, the lower left coordinate of the ‘SD-Box’ is defined as the
 233 mean peak time minus one standard deviation ($\mu_t - \sigma_t$) and the mean peak stage
 234 minus one standard deviation ($\mu_h - \sigma_h$) produced by all of the ensemble members.
 235 The upper right coordinate is defined as the mean peak time plus one standard
 236 deviation ($\mu_t + \sigma_t$) and the mean peak stage plus one standard deviation ($\mu_h +$
 237 σ_h) of all of the ensemble members. In principle, the ‘IQR-Box’ should contain
 238 25% (50% of the peak discharge times and 50% of the peak times) of all forecasts.
 239 In practice, it contained from 12.5% to 37.5%, due to the distribution of ensemble
 240 members (Zappa et al., 2013). Using the mean and the standard deviation (the ‘SD-
 241 Box’) results in a larger area, includes 46.60% of the ensemble forecasts (68.27%
 242 of peak water level times and 68.27% of the peak times) and has a greater chance
 243 of including the observed peaks.



244 d. **Include all forecasts with different lead times in the rectangle.** Descriptive
 245 statistics, such as the quartile deviation and the standard deviation, are susceptible
 246 to outliers when calculated using insufficient sample sizes. Adding extra ensemble
 247 members to produce more forecasts consumes computer resources. Yang et al.
 248 (2016) showed that the performance of NWP models is independent of the length
 249 of the lead time during typhoon events. Therefore, in order to expand the sample
 250 size, this study includes present (t) and previous forecasts ($t-1$, $t-2$, $t-3$... $t-n$, where
 251 n is the number of available forecasts when the system is initiated) to provide
 252 ensemble flow forecasts. As shown in the right panel of Figure 4, the green area
 253 illustrates the ‘SD-Box’. The black and gray solid dots represent the current and
 254 previous peak-flow forecasts, respectively.

255 5. RESULTS AND DISCUSSION

256 5.1 Performance evaluation criteria

257 **This study applied two performance measures, the root mean square error (RMSE)**
 258 **and the skill-spread ratio, to evaluate the proposed HEPS performance.** For a well-
 259 designed HEPS, the spread of ensemble forecasts will be large enough to cover the
 260 prediction uncertainty. This statement implies that the spread should be the same as or
 261 larger than the RMSE. The RMSE, which is commonly referred to as skill, measures
 262 the difference between the observations and the ensemble mean without considering



the direction. The closer the RMSE is to zero, the better the ensemble mean is as a
 forecast. The RMSE is defined as follows:

$$\text{RMSE} = \sqrt{(O_{\text{peak}} - \mu)^2} \quad (1)$$

$$\mu = \frac{1}{m} \sum_{i=1}^m P_{\text{peak},i} \quad (2)$$

$$\sigma = \sqrt{\frac{1}{m} \sum_{i=1}^m (P_{\text{peak},i} - \mu)^2} \quad (3)$$

where μ is the ensemble mean of ensemble peak-flow forecasts; O_{peak} is the observation
 of peak flow; $P_{\text{peak},i}$ is the prediction of peak flow of the i_{th} member; m is the number of
 ensemble members; and σ is the standard deviation of ensemble peak-flow forecasts.

The skill-spread score (hereinafter referred to as the score), which ranges from
 zero to infinity, is the ratio of the standard deviation of the ensemble peak-flow forecasts
 to the RMSE (Wilks, 2006). Scores less than one mean that the spread of the ensemble
 forecasts is large enough to cover the prediction uncertainty. It is defined as follows:

$$\text{Score} = \frac{\text{RMSE}}{\sigma} \quad (4)$$

5.2 Model calibration and validation

Two parameters in the proposed HEPS KW-GIUH model have been calibrated
 using in situ observations made during typhoon events. These parameters are the
 roughness coefficient for overland flow (n_0) and the roughness coefficient for channel



280 flow (n_c). The proposed HEPS used data from five rainfall gauges, including LTGX,
281 YSGZ, C1U610, C0U520 and C1U630 (see Figure 2 for locations), and the Thiessen
282 polygon method (Thiessen, 1911) to estimate the hourly spatial-average rainfall
283 intensities in order to provide rainfall input data to the KW-GIUH model. The
284 topographic data used in KW-GIUH are contained within a digital elevation model with
285 a resolution of 5 m obtained using aerial photographs. Kuo et al. (2016) used in situ
286 observations of flow discharges made at the Hsincheng and Yuanshan Bridges during
287 Typhoons Saola, Soulik, and Soudelor to calibrate the parameters of the KW-GIUH
288 model. Figure 5 shows that the percent errors in the peak discharges of the selected
289 typhoons were 4.59%, 2.07%, and -5.89% at the Hsincheng Bridge, and 14.88%, 5.28%,
290 and -3.05% at the Yuanshan Bridge, respectively. All of the errors in the peak times
291 were less than one hour. The results show that the KW-GIUH model is capable of
292 providing confident predictions for peak time, as well as peak discharge.

293 The WASH123D model adopted the most recent available cross-sectional
294 bathymetry of the Yilan River, which was measured in 2010, as its input topography
295 data. The upstream boundary of the model is set at the Hsincheng and Yuanshan Bridges,
296 and the downstream boundary of the model is set at the Kemalan Bridge. Field
297 measurements at the Hsincheng and Yuanshan Bridges from Kuo et al. (2016) and
298 observed water stages at the Kemalan Bridge were used as the upstream and



299 downstream boundary conditions, respectively. Field hourly records of water-stage at
300 the Zhongshan, Leawood, and Jhuangwei Bridges were used to calibrate the value of
301 Manning's roughness coefficient (n) in the WASH123D model and to validate the
302 performance of the model. Figure 6 shows that the percent errors in the peak stage for
303 Typhoons Saola, Soulik, and Soudelor, were 2.1%, 5.7%, and 10.6% at Zhongshan,
304 12.9% and 2.2% at Leawood, and 7.4%, 6.0%, and 2.1% at Jhuangwei, respectively.
305 There was one data gap at Leawood due to incomplete data collection during Typhoon
306 Soudelor. Nevertheless, all of the errors in the peak times were less than one hour. The
307 results show that WASH123D is capable of providing confident predictions of peak
308 times, as well as peak stages.

309 *5.3 Comparison of enveloping rectangles defined using the 'SD-Box' and the 'IQR-Box'* 310 *methods for supporting the interpretation of ensemble peak-flow results*

311 The proposed HEPS initiates when CWB issues a sea warning and ends when the
312 next ensemble forecast is six hours less than the left edge of the 'SD-Box'. In that regard,
313 93 forecasts are available for the four selected typhoons. Table 2 compares the forecast
314 peak stages and peak times between the 'SD-Box' and 'IQR-Box' approaches at the
315 Zhongshan, Leawood, and Zhuangwei Bridges. Scores were not calculated for the
316 Leawood Bridge during Typhoon Soudelor due to the lack of complete observations.
317 The scores that are less than one in the table are highlighted. These values indicate that



the spread of the ensemble members is large enough to contain the prediction uncertainty. The rectangles defined using the ‘IQR-Box’ method contain 33.3% (31/93) and 52.6% (49/93) of the observed peaks in stage and timing, respectively. Using the ‘SD-Box’ improves the capture rate to 51.6% (48/93) and 64.5% (60/93) for stage and timing, respectively. Among all of the forecasts, there is only one forecast for which the ‘IQR-Box’ score is less than one, and the score of the ‘SD-Box’ is not. This situation occurs at the Zhuangwei Bridge during Typhoon Soudelor. However, the score for the ‘SD-Box’ method is still very close to one (1.01), which means that it nearly captures the observed peak. Overall, the ‘SD-Box’ method yielded average scores of 1.18 for the peak stages and 1.08 for the peak times. In comparison with the ‘IQR-Box’ method, which yielded scores of 2.06 for the peak stages and 2.06 for the peak times, the results show that the enveloping rectangles defined using the ‘SD-Box’ method are more reliable during typhoon events.

5.4 Including all forecasts with different lead times during an event to expand the sample size

The sample size has a strong effect in terms of determining whether a result is statistically significant. In other words, the number of available ensemble members is important for both the ‘SD-Box’ and ‘IQR-Box’ methods. For example, the number of available ensemble members for each forecast ranged from 11 to 14 for the proposed



337 HEPS during operation. Thus, the descriptive statistics were calculated using
338 insufficient sample sizes (less than 30). The same issue exists in other studies that
339 employ HEPSs (e.g., Yang and Yang, 2014; Zappa et al., 2013). It is difficult to increase
340 the number of ensemble members used in HEPSs, due to the limited computational
341 resources that are available. Therefore, this study proposes a method for including
342 present and previous forecasts in order to expand the sample size during the estimation
343 process.

344 It must be shown that the forecast performance is independent of time before all
345 available forecasts can be included in the estimation process. The time of concentration
346 of the peak flow at the Zhongshan Bridge is approximately 4 hours. This study
347 calculated the error in the maximum 4-hour rainfall between the average forecasts and
348 the average observations at the watershed upstream of the Zhongshan Bridge. Figure 7
349 shows that there is no obvious trend in the errors in stage and timing, regardless of the
350 length of the lead time. The correlation coefficients were -0.09 and 0.11, respectively,
351 and these values indicate that no significant correlations exist between errors in stage
352 or timing on the one hand and lead time on the other. For example, the best and worst
353 forecasts during Typhoon Dujuan in terms of stage error were the 1st and 5th forecasts,
354 respectively. However, the 6th forecast was better than the 5th, which implies that there
355 is no trend in the cascading forecasting process. Based on these results, this study



356 assumed that the performance of the HEPS is independent of lead time during typhoon
 357 events. Therefore, it is reasonable to include all available forecasts during an event to
 358 expand the sample size.

359 Figure 8 illustrates the comparisons between using the ‘SD-Box’ method with one
 360 forecast and using the ‘SD-Box’ method including all available forecasts (hereinafter
 361 indicated as ‘SD-Box Single’ and ‘SD-Box All’) at the Zhongshan Bridge. The
 362 performance of ‘SD-Box All’ was more consistent than that of ‘SD-Box Single’ in terms
 363 of both stage and timing. For example, the scores for stage during Typhoon Soudelor
 364 ranged from 0 to 5 when the ‘SD-Box Single’ method was used, but they were below
 365 or close to 1 with ‘SD-Box All’. The results showed that the inclusion of all available
 366 forecasts in the calculation process decreased the variation among the forecasts; in other
 367 words, the uncertainty of the forecasts decreased. Figure 9 illustrates the scores of all
 368 of the forecasts for the different typhoon events. The ‘SD-Box Single’ contained 47.1%
 369 of the observed peaks in terms of stage (37.3% + 9.8%), whereas ‘SD-Box All’
 370 contained 63.7% (57.8% + 5.9%) of the observed peaks. Furthermore, the ‘SD-Box
 371 Single’ contained 58.9% (37.3% + 21.6%) of the observed peaks in terms of timing,
 372 whereas ‘SD-Box All’ contained 71.5% (57.8% + 13.7%). The results show that the
 373 ‘SD-Box All’ method can capture more of the observed peaks in terms of both stage



374 and timing. In particular, ‘SD-Box All’ improved the forecast performance and
375 increased the capture rate from 37.3% to 57.8% for both stage and timing.

376 6. CONCLUSIONS

377 This study proposed a HEPS that employs NWP models to perform rainfall
378 forecasts and hydrologic models to produce ensemble flood forecasts during typhoon
379 events. Because the communication of ensemble forecasts is critical for helping end-
380 users to respond, a modified version of the ‘Peak-Box’ visualization method, which was
381 originally described by Zappa et al. (2013), was also proposed to support the
382 interpretation of ensemble forecast results for operational purposes. Four typhoon
383 events during the period 2012-2015 and observations collected in the Yilan
384 Experimental Watershed were used to evaluate the performance of these techniques. A
385 total of 93 forecasts and two performance measures were considered. The results
386 showed that the proposed HEPS is able to provide flood forecasts during the selected
387 typhoon events. In addition, the ‘SD-Box’ visualization approach, which considers the
388 mean and the standard deviation instead of the 25th and 75th percentiles, captured more
389 of the observed peaks during typhoon events. The average skill-spread scores of the
390 ‘SD-Box’ method for the selected events were 1.18 and 1.08 in terms of stage and
391 timing, respectively. These results represent a significant improvement over the original
392 ‘Peak-Box’ method, which resulted in scores of 2.06 for both peak stage and peak



393 timing. Scores of less than one indicate that the spread of the ensemble forecasts is large
394 enough to contain the prediction uncertainty. Since the average score achieved by the
395 ‘SD-Box’ method was close to one, it has been shown to be more reliable than the
396 original ‘Peak-Box’ method during typhoon events. The results satisfy the statement
397 “One of the main objectives of ensemble flood forecasts is the representation of the full
398 spectrum of forecast uncertainty and/or predictability in [the] form of different
399 hydrological responses to the input of the various members obtained from an
400 atmospheric EPS” made by Zappa et al. (2013).

401 Descriptive statistics, such as the quartile deviation and the standard deviation, are
402 susceptible to outliers when calculated using an insufficient number of observations.
403 Adding more ensemble members is expensive in terms of computer resources. This
404 study proposed a method that enables increasing the sample size, leading to statistically
405 significant results. This method involves including present and previous available
406 forecasts in the calculation process. For example, the proposed HEPS generated 11
407 available ensemble members at each forecast during Typhoon Dujuan. By including all
408 of the present and previous available forecasts (the ‘SD-Box All’ method), the sample
409 size increased to 22 for the second forecast, 33 for the third forecast, and so on. The
410 results showed that the ‘SD-Box All’ made more consistent predictions. This result can
411 be explained by the inclusion of all available forecasts in the calculation process



412 decreasing the uncertainty of the forecasts. As a result, the rectangles defined by the
413 ‘SD-Box All’ method contained 57.8% of the observed peaks in stage and timing.
414 Coughlan de Perez et al. (2016) suggested that a HEPS that produces a false alarm rate
415 below 50% is tolerable for decision makers in terms of the economic and practical
416 consequences of taking action. However, this study assumed that the forecast
417 performance of the proposed HEPS is independent of the length of the lead time and
418 conducted an experiment to prove it. Other studies, such as that of Zappa et al. (2013),
419 have claimed that the most accurate forecasts were obtained for lead times of two or
420 more days. Such statements imply that the performance of HEPSs do not improve with
421 shorter lead times or are independent of lead time, and Yang et al. (2016) found that the
422 best performance is obtained before a typhoon makes landfall. This assumption is still
423 susceptible to the topography of the applied area and the type of extreme event being
424 considered. Further investigation of various conditions must be performed before firm
425 conclusions can be drawn. Regardless, the proposed HEPS and the modified
426 visualization approach have been shown to produce convincing peak-stage and peak-
427 timing forecasts for operational purposes during a typhoon.

428 AUTHOR CONTRIBUTION

429 Ya-Chi Chang, Mei-Ying Lin, Jui-Yi Ho calibrated and verified the parameters of
430 WASH123D, POM and KW-GIUH models. Cheng-Hsin Chen dealt with the data
431 processing of the models and performed the simulations. Sheng-Chi Yang and Ya-Chi



432 Chang analyzed the results of HEPS and developed a new approach for improved
433 interpretation during typhoon events. Sheng-Chi Yang, Tsun-Hua Yang, Ya-Chi Chang
434 and Kwan-Tun Lee prepared the manuscript with contributions from all co-authors.

435 ACKNOWLEDGMENTS

436 The authors thank the Water Resources Agency of Taiwan for providing the
437 hydrological observations from the rainfall gauges and water level stations in the Yilan
438 River Basin. Thanks are also due to the Taiwan Typhoon and Flood Research Institute
439 and the National Applied Research Laboratories for providing the results from the
440 Taiwan Cooperative Precipitation Ensemble Forecast Experiment and historical records
441 from the Yilan Experimental Watershed. This work was supported by the Ministry of
442 Science and Technology, R.O.C., under grant MOST 105-3011-F-492-009.

443 REFERENCES

- 444 Bartholmes, J. C., Thielen, J., Ramos, M. H., and Gentilini, S.: The european flood alert
445 system EFAS-Part 2: Statistical skill assessment of probabilistic and deterministic
446 operational forecasts, *Hydrology and Earth System Sciences*, 13, 141-153, 2009.
- 447 Blumberg, A. F. and Mellor, G. L.: A Description of a Three-Dimensional Coastal
448 Ocean Circulation Model, in *Three-Dimensional Coastal Ocean Models*,
449 American Geophysical Union, Washington, D.C., 1987.
- 450 Bruen, M., Krahe, P., Zappa, M., Olsson, J., Vehvilainen, B., Kok, K., and Daamen, K.:
451 Visualizing flood forecasting uncertainty: some current European EPS platforms-
452 COST731 working group 3, *Atmospheric Science Letters*, 11, 92-99, 2010.
- 453 Chiou, M. D.: Characteristic and numerical simulation of astronomic tide and storm
454 surge in Taiwan water, Ph. D., Department of Hydraulic and Ocean Engineering,
455 National Cheng Kung University, Tainan, Taiwan, 135 pp., 2010.
- 456 Cloke, H. L. and Pappenberger, F.: Ensemble flood forecasting: A review, *J. Hydrol.*,
457 375, 613-626, 2009.
- 458 Coughlan de Perez, E., van den Hurk, B., van Aalst, M. K., Amuron, I., Bamanya, D.,
459 Hauser, T., Jongman, B., Lopez, A., Mason, S., Mender de Suarez, J.,



- 460 Pappenberger, F., Rueth, A., Stephens, E., Suarez, P., Wagemaker, J., and Zsoter,
461 E.: Action-based flood forecasting for triggering humanitarian action, *Hydrology*
462 *and Earth System Sciences*, 20, 3549-3560, 2016.
- 463 Cuo, L., Pagano, T.C. and Wang, Q.J.: A review of quantitative precipitation forecasts
464 and their use in short-to medium-range streamflow forecasting, 12, 713-728, 2011.
- 465 Demeritt, D., Cloke, H., Pappenberger, F., Thielen, J., Bartholmes, J., and Ramos, M.-
466 H.: Ensemble predictions and perceptions of risk, uncertainty, and error in flood
467 forecasting, *Environmental Hazards*, 7, 115-127, 2007.
- 468 Demeritt, D., Nobert, S., Cloke, H., and Pappenberger, F.: Challenges in
469 communicating and using ensembles in operational flood forecasting,
470 *Meteorological applications*, 17, 209-222, 2010.
- 471 Frick, J. and Hegg, C.: Can end-users' flood management decision making be improved
472 by information about forecast uncertainty?, *Atmospheric Research*, 100, 296-303,
473 2011.
- 474 Fundel, F. and Zappa, M.: Hydrological ensemble forecasting in mesoscale catchments:
475 Sensitivity to initial conditions and value of reforecasts, *Water Resources*
476 *Research*, 47, W09520, 2011.
- 477 Hostache, R., Matgen, P., Montanari, A., Montanari, M., Hoffmann, L., and Pfister, L.:
478 Propagation of uncertainties in coupled hydro-meteorological forecasting systems:
479 A stochastic approach for the assessment of the total predictive uncertainty,
480 *Atmospheric Research*, 100, 263-274, 2011.
- 481 Hsiao, L. F., Yang, M. J., Lee, C. S., Kuo, H. C., Shih, D. S., Tsai, C. C., Wang, C. J.,
482 Chang, L. Y., Chen, D. Y. C., and Feng, L.: Ensemble forecasting of typhoon
483 rainfall and floods over a mountainous watershed in Taiwan, *J. Hydrol.*, 506, 55-
484 68, 2013.
- 485 Huang Jr, C., Yu, C. K., Lee, J. Y., Cheng, L. W., Lee, T. Y., and Kao, S. J.: Linking
486 typhoon tracks and spatial rainfall patterns for improving flood lead time
487 predictions over a mesoscale mountainous watershed, *Water Resources Research*,
488 48, 2012.
- 489 Jang, J. H., Yu, P. S., Yeh, S. H., Fu, J. C., and Huang, C. J.: A probabilistic model for
490 real-time flood warning based on deterministic flood inundation mapping,
491 *Hydrological processes*, 26, 1079-1089, 2012.
- 492 Jaun, S., Ahrens, B., Walser, A., Ewen, T., and Schär, C.: A probabilistic view on the



- 493 August 2005 floods in the upper Rhine catchment, Natural Hazards and Earth
494 System Science, 8, 281-291, 2008.
- 495 Kuo, C. W., Hong, J. H., Wang, H. W., Wang, Y. C., Tsun, S. C., and Li, S. C.:
496 Comparisons of velocity profile extrapolation methods for moving-boat ADCP
497 flow measurements, Taiwan Water Conservancy, 35-46, 2016.
- 498 Lee, K. T., Chang, C. H., Yang, M. S., and Yu, W. S.: Reservoir attenuation of floods
499 from ungauged watersheds, Hydrological Sciences Journal, 46, 349-362, 2001.
- 500 Lee, K. T., Chung, Y. R., Lau, C. C., Meng, C. C., and Chiang, S.: A windows-based
501 inquiry system for design discharge based on geomorphic runoff modeling,
502 Computers and Geosciences, 32, 203-211, 2006.
- 503 Lee, K. T. and Yen, B. C.: Geomorphology and kinematic-wave-base hydrograph
504 derivation, Journal of Hydraulic Engineering ASCE, 123, 73-80, 1997.
- 505 Li, M. H., Yang, M. J., Soong, R., and Huang, H. L.: Simulating typhoon floods with
506 gauge data and mesoscale-modeled rainfall in a mountainous watershed, Journal
507 of Hydrometeorology, 6, 306-323, 2005.
- 508 Ou, S., Liu, J., Tsai, C., and Hsu, T.: Numerical studies of typhoon-induced storm surge
509 using POM and finite element depth-averaged model in Taiwan, Chinese-German
510 Joint Symposium on Hydraulic and Ocean Engineering, Darmstadt, 2008.
- 511 Pagano, T. C., Wood, A. W., Ramos, M.-H., Cloke, H. L., Pappenberger, F., Clark, M.
512 P., Cranston, M., Kavetski, D., Mathevet, T., and Sorooshian, S.: Challenges of
513 operational river forecasting, Journal of Hydrometeorology, 15, 1692-1707, 2014.
- 514 Palmer, T. N.: A nonlinear dynamical perspective on model error: A proposal for non-
515 local stochastic-dynamic parametrization in weather and climate prediction
516 models, Quarterly Journal of the Royal Meteorological Society, 127, 279-304,
517 2001.
- 518 Pappenberger, F., Beven, K. J., Hunter, N. M., Bates, P. D., Gouweleeuw, B. T., Thielen,
519 J., and de Roo, A. P. J.: Cascading model uncertainty from medium range weather
520 forecasts (10 days) through a rainfall-runoff model to flood inundation predictions
521 within the European Flood Forecasting System (EFFS), Hydrology and Earth
522 System Sciences, 9, 381-393, 2005.
- 523 Pappenberger, F., Cloke, H. L., Persson, A., and Demeritt, D.: HESS Opinions On
524 forecast (in)consistency in a hydro-meteorological chain: curse or blessing?,
525 Hydrology and Earth System Sciences, 15, 2011.



- 526 Pappenberger, F., Stephens, E., Thielen, J., Salamon, P., Demeritt, D., van Andel, S. J.,
527 Wetterhall, F., and Alfieri, L.: Visualizing probabilistic flood forecast information:
528 expert preferences and perceptions of best practice in uncertainty communication,
529 Hydrological Processes, 27, 132-146, 2013.
- 530 Ramos, M. H., Mathevet, T., Thielen, J., and Pappenberger, F.: Communicating
531 uncertainty in hydro - meteorological forecasts: mission impossible?,
532 Meteorological Applications, 17, 223-235, 2010.
- 533 Renard, B., Kavetski, D., Kuczera, G., Thyer, M., and Franks, S. W.: Understanding
534 predictive uncertainty in hydrologic modeling: The challenge of identifying input
535 and structural errors, Water Resources Research, 46, W05521, 2010.
- 536 Rossa, A., Liechti, K., Zappa, M., Bruen, M., Germann, U., Haase, G., Keil, C., and
537 Krahe, P.: The COST 731 Action: A review on uncertainty propagation in
538 advanced hydro-meteorological forecast systems, Atmospheric Research, 100,
539 150-167, 2011.
- 540 Shih, D. S., Yeh, G. T., and Cheng, J. R. C.: Model assessments of precipitation with a
541 unified regional circulation rainfall and hydrological watershed model, Journal of
542 Hydrologic Engineering ASCE, 17, 43-54, 2012.
- 543 Thielen, J., Bartholmes, J., Ramos, M. H., and de Roo, A. P. J.: The European Flood
544 Alert System; Part 1: Concept and development, Hydrology and Earth System
545 Sciences, 13, 125-140, 2009.
- 546 Thiessen, A. H.: Precipitation averages for large areas, Monthly Weather Review, 39,
547 1082-1084, 1911.
- 548 Thirel, G., Martin, E., Mahfouf, J. F., Massart, S., Ricci, S., and Habets, F.: A past
549 discharges assimilation system for ensemble streamflow forecasts over France-
550 Part 1: Description and validation of the assimilation system, Hydrology and Earth
551 System Sciences, 14, 1623-1637, 2010.
- 552 Todini, E.: Predictive uncertainty assessment in real time flood forecasting. In:
553 Uncertainties in Environmental Modelling and Consequences for Policy Making,
554 Baveye, P. C., Laba, M., and Mysiak, J. (Eds.), Springer, Dordrecht, Netherlands,
555 2009.
- 556 Wilks, D. S.: Statistical Methods in the Atmospheric Sciences, Elsevier, Amsterdam,
557 2006.
- 558 Yang, S. C. and Yang, T. H.: Uncertainty assessment: Reservoir inflow forecasting with

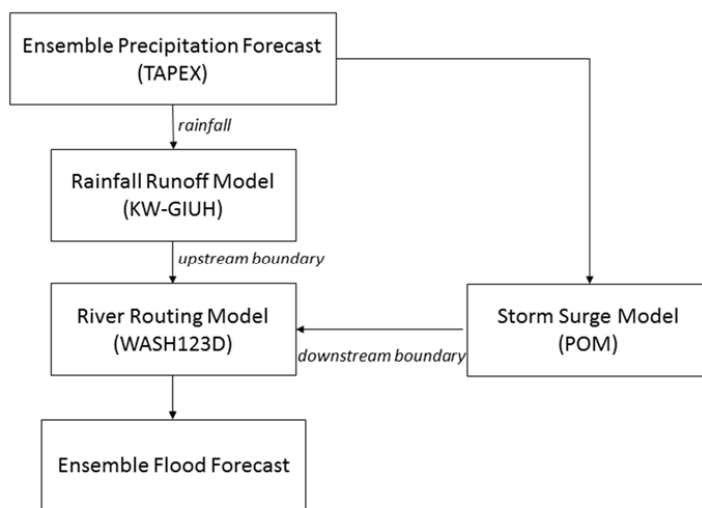


- 559 ensemble precipitation forecasts and HEC-HMS, *Advances in Meteorology*, 2014,
560 2014.
- 561 Yang, T. H., Hwang, G. D., Tsai, C.-C., and Ho, J.-Y.: Using rainfall thresholds and
562 ensemble precipitation forecasts to issue and improve urban inundation alerts,
563 *Hydrology and Earth System Sciences*, 20, 4731, 2016.
- 564 Yeh, G. T., Cheng, H. P., Cheng, J. R., and Lin, J. H.: A numerical model to simulate
565 flow and contaminant and sediment transport in watershed systems (WASH12D).
566 Technical Rep. CHL-98-15, Waterways Experiment Station, U. S. Army Corps of
567 Engineers, Vicksburg, MS 39180-6199., 1998. 1998.
- 568 Yeh, G. T., Huang, G. B., Zhang, F., Cheng, H. P., and Lin, H. C.: WASH123D: A
569 numerical model of flow, thermal transport, and salinity, sediment, and water
570 quality transport in watershed systems of 1-D stream-river network, 2-D overland
571 regime, and 3-D subsurface media. Technical Rep. submitted to EPA, Dept. of
572 Civil and Environmental Engineering, 2006.
- 573 Yeh, G. T., Shih, D. S., and Cheng, J. R. C.: An integrated media, integrated processes
574 watershed model, *Computers and Fluids*, 45, 2-13, 2011.
- 575 Zappa, M., Beven, K. J., Bruen, M., Cofino, A. S., Kok, K., Martin, E., Nurmi, P.,
576 Orfila, B., Roulin, E., Schroter, K., Seed, A., Szturc, J., Vehvilainen, B., Germann,
577 U., and Rossa, A.: Propagation of uncertainty from observing systems and NWP
578 into hydrological models: COST-731 Working Group 2, *Atmospheric Science*
579 *Letter*, 11, 83-91, 2010.
- 580 Zappa, M., Fundel, F., and Jaun, S.: A 'Peak-Box' approach for supporting interpretation
581 and verification of operational ensemble peak-flow forecasts, *Hydrological*
582 *Processes*, 27, 117-131, 2013.
- 583 Zappa, M., Jaun, S., Germann, U., Walser, A., and Fundel, F.: Superposition of three
584 sources of uncertainties in operational flood forecasting chains, *Atmospheric*
585 *Research*, 100, 246-262, 2011.



586

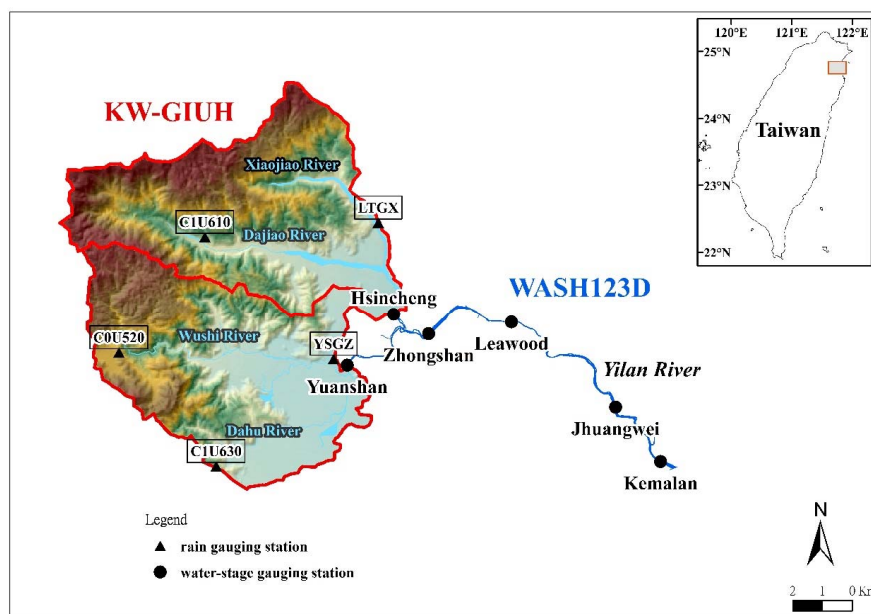
FIGURES



587

588 **Figure 1** Flowchart describing the flow of data processing within the Yilan River
 589 HEPS.

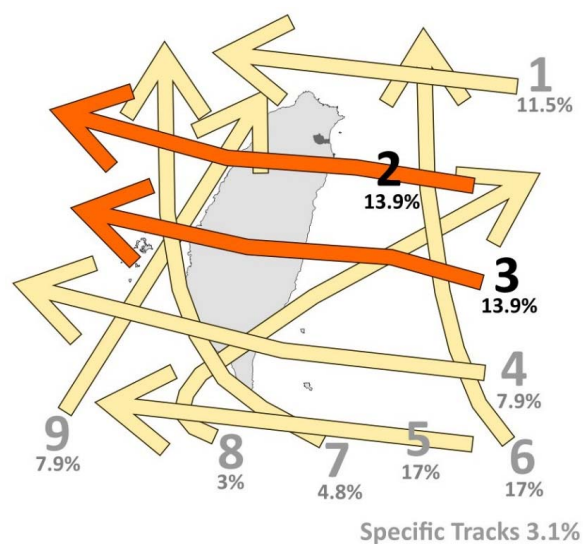
590



591

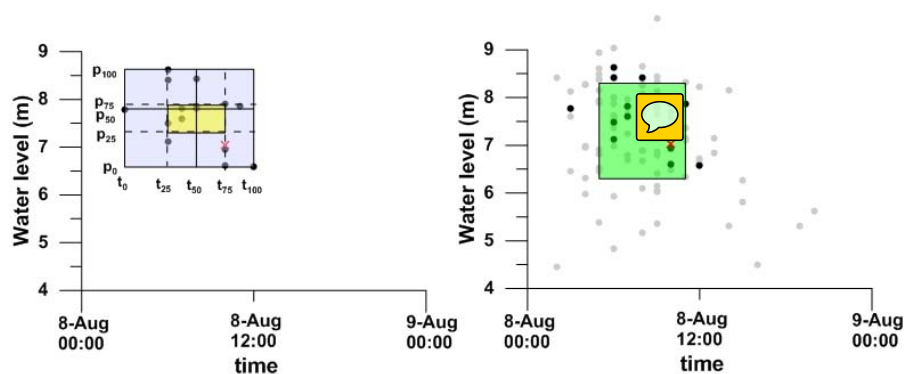
592 **Figure 2** Study area and locations of streamflow gauges. Black dots and triangles
 593 indicate the locations of water-stage gauging stations and rain gauge stations,
 594 respectively.

595



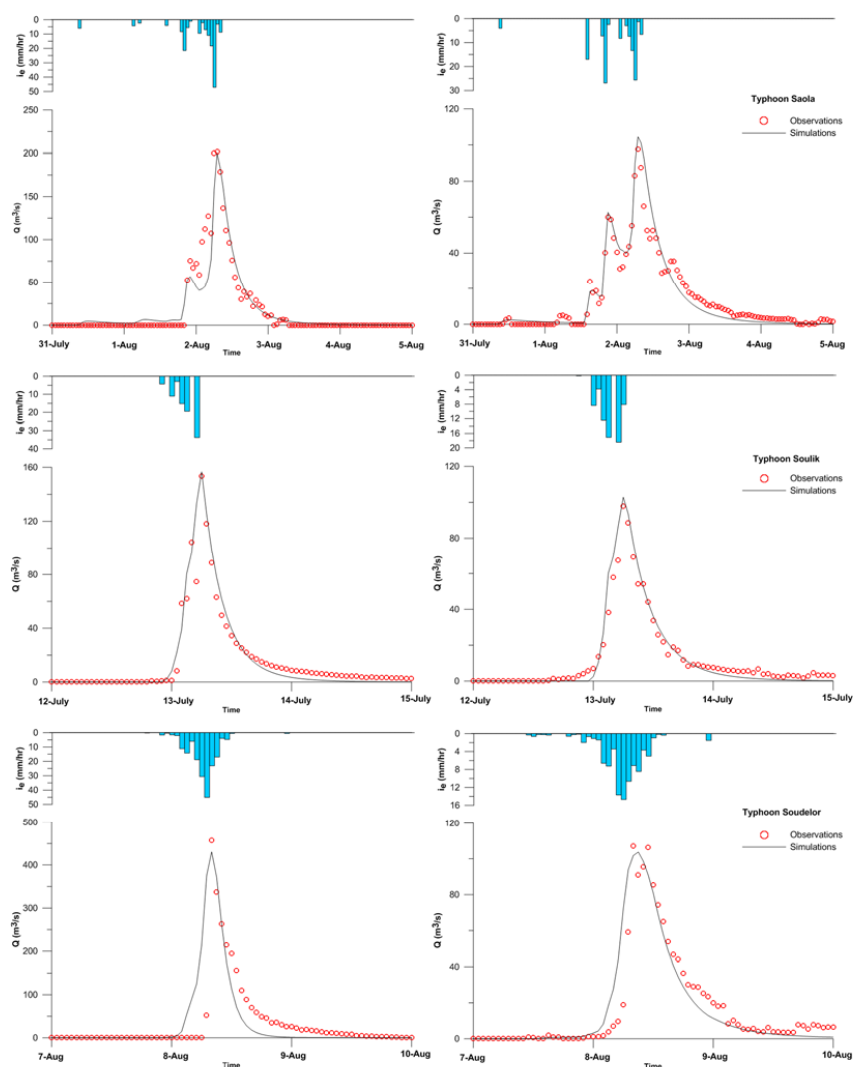
Redrawn from Kuo et al. (2012)

596 **Figure 3** Schematic diagram showing the tracks of typhoons invading Taiwan. The
 597 percentages shown in the figure are the statistical results from 1958 through 2006
 598 obtained from the Central Weather Bureau (CWB). The dark gray polygon located in
 599 northern Taiwan indicates the Yilan River catchment. Type-2 and Type-3 typhoons
 600 bring heavy rainfall to the Yilan River catchment.

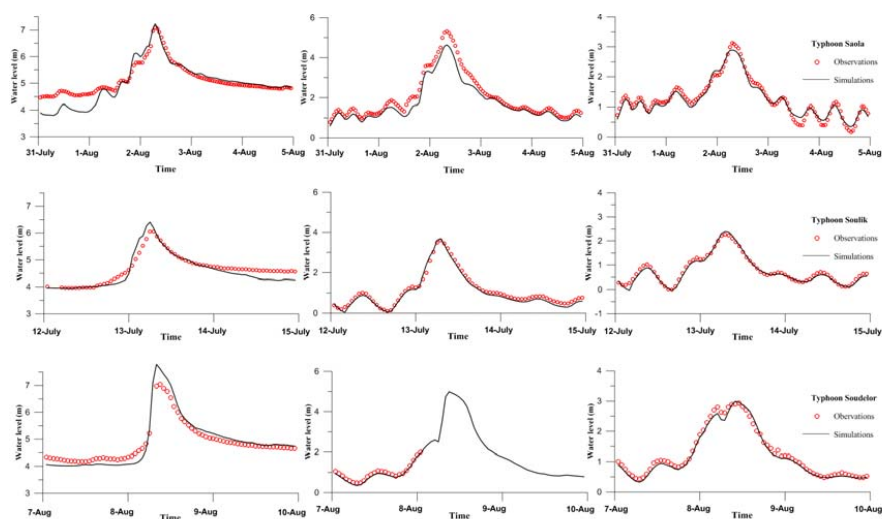


601

602 **Figure 4** The left panel shows a graphical explanation of the 'Peak-Box' approach.
 603 The outer rectangle is the 'Peak-Box,' and the internal rectangle (the yellow area) is
 604 the 'IQR-Box'. The solid dots represent all of the ensemble forecasts. The right panel
 605 shows a graphic explanation of the proposed extension of the 'Peak-Box' approach.
 606 The enveloping rectangle is the 'SD-Box' (the green area). The solid black and gray
 607 dots represent current and previous peak-flow forecasts, respectively.



608 **Figure 5** Comparison of simulated discharges (red circles) and recorded discharges
 609 (solid lines) for model calibration (Typhoons Saola and Soulik) and validation
 610 (Typhoon Soudelor) experiments at Hsinsheng (left) and Yuanshen (right). The blue
 611 bars are the hourly spatial-average rainfall intensities measured in the watershed
 612 upstream of Hsinsheng and Yuanshen.

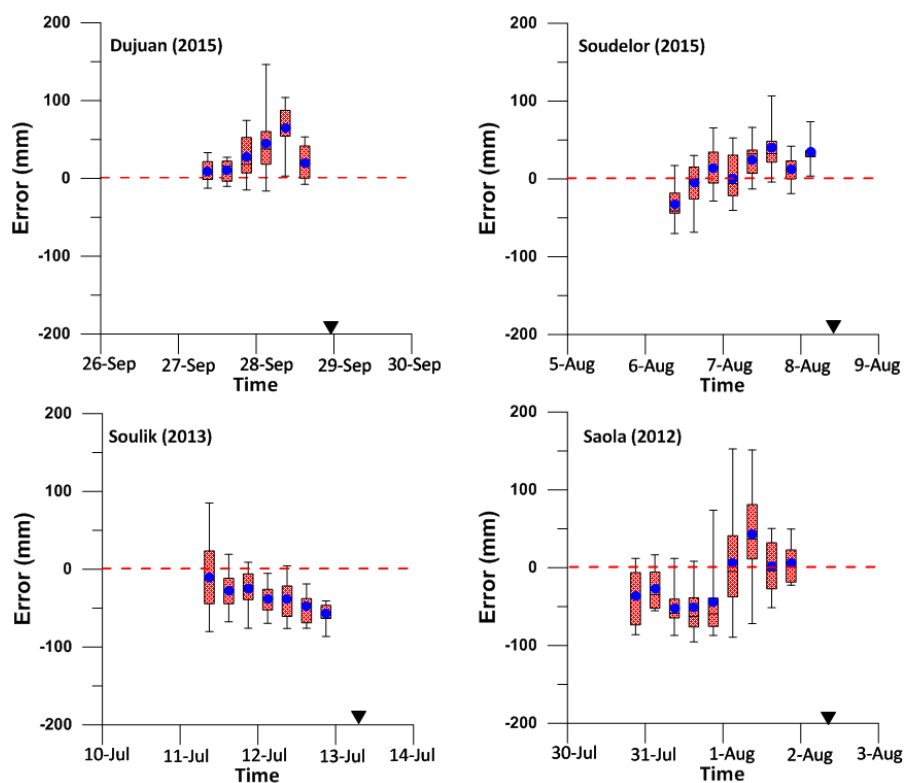


613

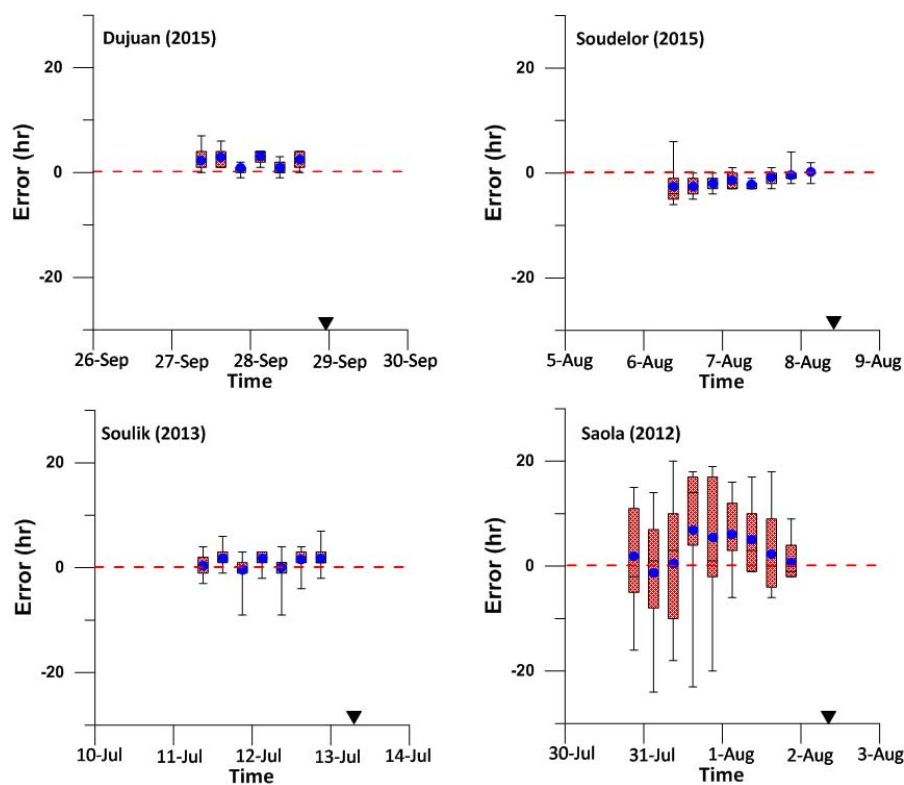
614 **Figure 6** Comparison of simulated (red circles) and recorded (solid lines) water levels
 615 for model calibration (Typhoons Saola and Soulik) and validation (Typhoon Soudelor)
 616 experiments at Zhongshan (left), Leawood (central) and Jhungwei (right).



(a) Magnitude error of maximum 4-hour rainfall



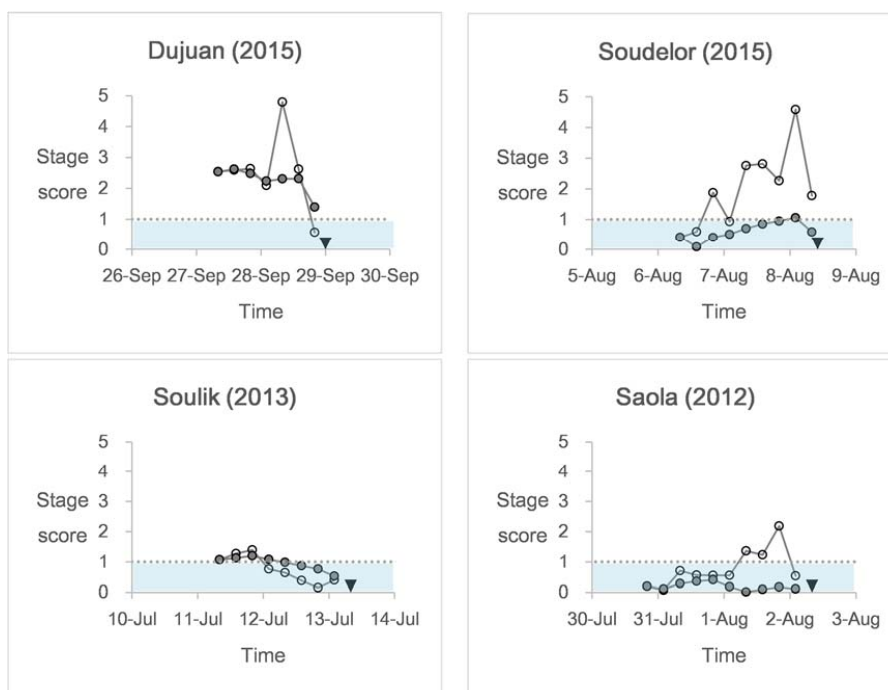
(b) Timing error of maximum 4-hour rainfall



617 **Figure 7** Box-and-whisker plot at the watershed upstream of the Zhongshan Bridge
 618 during the four selected typhoon events. The blue dots indicate the ensemble means.
 619 The inverted triangles indicate the time of occurrence of the maximum 4-hour rainfall.
 620 The results show that there is no obvious trend in lead time for the errors in either the
 621 stage or timing.



(a) Scores for peak-stage forecasts



(b) Scores in peak-timing forecasts

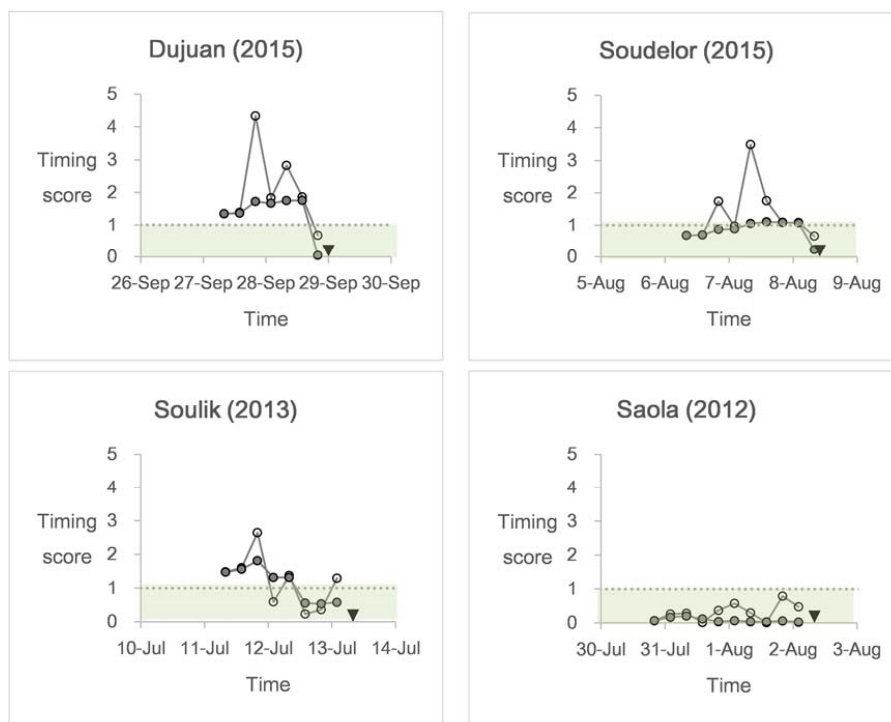
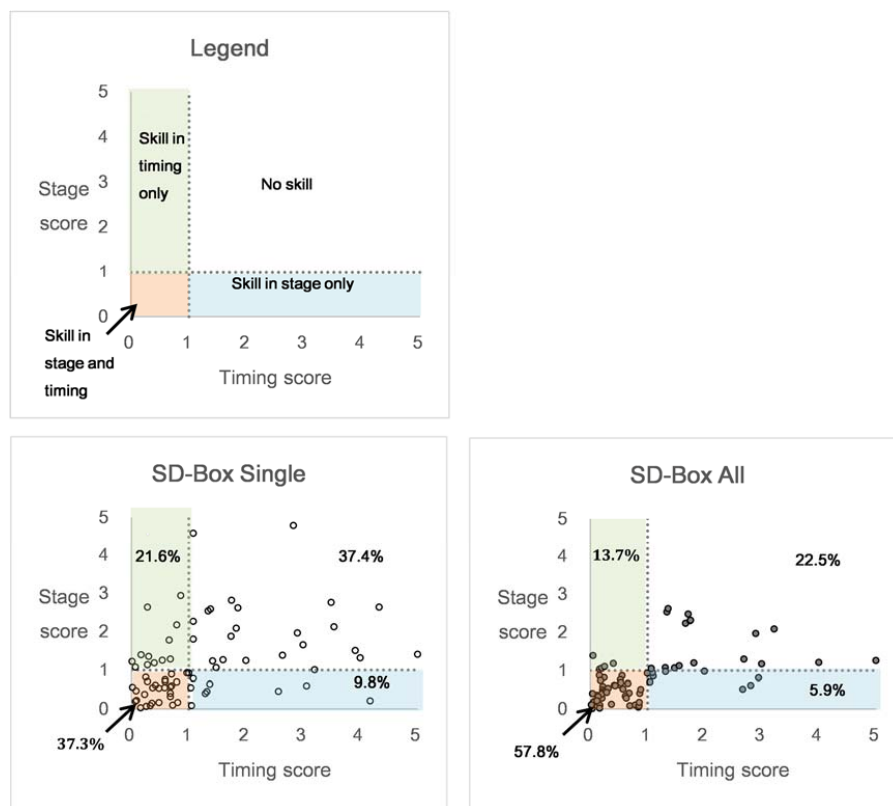


Figure 8 The scores of the single ('SD-Box Single') and accumulating ('SD-Box All') methods at the Zhongshan Bridge during the four selected typhoon events. The inverted triangles indicate the time of occurrence of the observed peak stage. The results show that the performance of the 'SD-Box All' method (solid circles) was more stable than that of the 'SD-Box Single' method (open circles) in terms of both stage and timing.



628

629 **Figure 9** Comparison of scores obtained for ‘SD-Box Single’ and ‘SD-Box All’. The
 630 results show that the ‘SD-Box All’ approach significantly improves the performance
 631 compared with the results obtained using the ‘SD-Box Single’ method.



632

TALBLES

633 **Table 1** All typhoons that invaded Taiwan during 2012 through 2015. A total of four
 634 typhoons of Type-2 and Type-3, namely, Saola in 2012, Soulik in 2013, Soudelor in
 635 2015, and Dujuan in 2015, were selected to calibrate the system and test the
 636 performance in this study. Typhoon Matmo, a Type-3 typhoon that occurred in 2014,
 637 was not selected due to its weak typhoon intensity.

Typhoon	Track	Intensity	Warning Period
DUJUAN	2	3	27-29 September 2015
GONI	—	—	20-23 August 2015
SOUDELOR	3	3	6-9 August 2015
LINFA	—	—	6-9 July 2015
CHAN-HOM	—	2	9-11 July 2015
NOUL	—	—	10-11 May 2015
FUNG-WONG	Special	—	19-22 September 2014
MATMO	3	—	21-23 July 2014
HAGIBIS	—	3	14-15 Jun 2014
FITOW	1	—	4-7 October 2014
USAGI	5	3	19-22 September 2013
KONG-REY	6	—	27-29 August 2013
TRAMI	1	—	20-22 August 2013
CIMARON	—	—	17-18 July 2013
SOULIK	2	1	11-13 July 2013
JELAWAT	—	—	27-28 September 2012
TEMBIN	Special	—	21-25 August 2012
		—	26-28 August 2012
KAI-TAK	—	1	14-15 August 2012
HAIKUI	—	—	6-7 August 2012
SAOLA	2	4	30 July - 3 August 2012
DOKSURI	—	—	28-29 Jun 2012
TALIM	9	—	19-21 Jun 2012

638

(Source: Central Weather Bureau, Taiwan)



Table 2 Comparisons of scores in peak stage and peak time between the ‘IQR-Box’ and ‘SD-Box’ approaches. Scores less than one (highlighted) indicate that the enveloping rectangle did contain the observed peak.

(a) Scores in peak-stage forecasts

Location/Typhoon	Method	Forecast									
		1	2	3	4	5	6	7	8	9	10
Zhongshan Bridge											
Dujuan (2015)	SD-Box	2.54	2.59	2.64	2.09	4.79	2.62	0.57	—	—	—
	IQR-Box	2.83	3.78	3.30	4.53	14.03	2.87	1.07	—	—	—
Soudelor (2015)	SD-Box	0.41	0.60	1.88	0.93	2.76	2.82	2.27	4.59	1.78	—
	IQR-Box	0.22	1.26	2.20	1.14	3.39	7.00	4.07	10.60	2.58	—
Soulik (2013)	SD-Box	1.07	1.27	1.39	0.76	0.64	0.38	0.15	0.40	—	—
	IQR-Box	1.86	1.76	1.94	1.29	0.87	0.36	0.65	0.56	—	—
Saola (2012)	SD-Box	0.20	0.07	0.71	0.56	0.55	0.55	1.36	1.23	2.18	0.54
	IQR-Box	0.14	0.01	1.81	0.79	1.70	1.42	3.66	1.90	2.45	0.48
Leawood Bridge											
Dujuan (2015)	SD-Box	1.21	1.27	1.75	1.24	3.48	1.48	1.67	—	—	—
	IQR-Box	1.10	2.29	2.17	2.98	11.15	1.84	3.23	—	—	—
Soudelor (2015)	SD-Box	—	—	—	—	—	—	—	—	—	—
	IQR-Box	—	—	—	—	—	—	—	—	—	—
Soulik (2013)	SD-Box	0.79	0.95	1.06	0.36	0.20	0.10	0.27	0.54	—	—
	IQR-Box	1.76	1.79	2.06	0.75	0.31	0.16	0.09	0.76	—	—
Saola (2012)	SD-Box	0.93	1.25	1.66	1.32	1.41	0.16	0.29	0.22	0.04	1.36
	IQR-Box	1.14	2.12	2.71	1.60	2.51	0.00	1.32	0.01	0.28	1.36
Zhuangwei Bridge											
Dujuan (2015)	SD-Box	1.97	2.13	0.60	0.21	0.46	1.51	2.94	—	—	—
	IQR-Box	2.76	2.88	0.73	0.35	1.62	1.93	4.29	—	—	—
Soudelor (2015)	SD-Box	1.19	0.17	0.45	0.10	1.01	1.24	0.55	1.81	2.64	—
	IQR-Box	1.47	0.23	0.31	0.00	0.87	3.30	0.85	3.03	3.69	—
Soulik (2013)	SD-Box	0.62	0.71	0.79	0.17	0.03	0.32	0.47	0.90	—	—
	IQR-Box	1.45	1.53	1.77	0.49	0.00	0.40	0.45	1.18	—	—
Saola (2012)	SD-Box	0.82	1.08	1.40	1.14	1.26	0.09	0.70	0.09	0.22	1.29
	IQR-Box	1.06	2.39	2.55	1.57	3.42	0.39	1.77	0.37	0.03	1.39



644 (b) Scores in peak-timing forecasts

Location/Typhoon	Method	Forecast									
		1	2	3	4	5	6	7	8	9	10
Zhongshan Bridge											
Dujuan (2015)	SD-Box	1.34	1.38	4.33	1.83	2.83	1.86	0.68	—	—	—
	IQR-Box	3.67	3.00	9.00	2.00	3.00	1.67	0.94	—	—	—
Soudelor (2015)	SD-Box	0.68	0.70	1.74	0.97	3.49	1.75	1.08	1.08	0.66	—
	IQR-Box	1.00	1.67	3.00	1.00	7.00	2.00	—	3.00	5.40	—
Soulik (2013)	SD-Box	1.48	1.60	2.64	0.59	1.37	0.23	0.36	1.29	—	—
	IQR-Box	3.00	3.57	4.00	1.00	2.00	1.00	1.00	2.33	—	—
Saola (2012)	SD-Box	0.07	0.26	0.28	0.02	0.37	0.58	0.30	0.01	0.79	0.48
	IQR-Box	0.10	0.29	0.81	0.18	0.67	1.14	0.33	0.11	1.00	0.56
Leawood Bridge											
Dujuan (2015)	SD-Box	0.46	0.11	1.69	0.32	2.24	0.58	0.71	—	—	—
	IQR-Box	1.00	0.33	3.00	0.20	3.00	0.60	1.00	—	—	—
Soudelor (2015)	SD-Box	—	—	—	—	—	—	—	—	—	—
	IQR-Box	—	—	—	—	—	—	—	—	—	—
Soulik (2013)	SD-Box	0.40	1.17	1.96	0.39	0.71	0.11	0.09	0.96	—	—
	IQR-Box	1.18	5.00	3.00	1.00	1.00	1.00	1.00	1.50	—	—
Saola (2012)	SD-Box	0.04	0.09	0.34	0.17	0.04	0.11	0.46	0.07	0.67	0.53
	IQR-Box	0.29	0.10	0.76	0.22	0.53	0.88	0.50	0.00	0.80	1.00
Zhuangwei Bridge											
Dujuan (2015)	SD-Box	2.90	3.54	3.06	4.17	2.57	3.91	0.86	—	—	—
	IQR-Box	6.33	11.00	5.00	7.00	3.00	4.20	1.13	—	—	—
Soudelor (2015)	SD-Box	0.40	0.48	1.32	0.72	3.20	1.42	1.04	1.08	0.28	—
	IQR-Box	0.50	1.00	1.67	1.00	3.00	2.00	3.00	3.00	0.00	—
Soulik (2013)	SD-Box	0.42	0.59	1.08	0.81	0.16	0.68	0.08	0.70	—	—
	IQR-Box	0.33	1.00	2.00	3.00	0.14	3.00	1.00	1.00	—	—
Saola (2012)	SD-Box	0.25	0.07	0.17	0.28	0.54	1.05	0.79	0.33	0.09	0.68
	IQR-Box	0.72	0.50	0.00	3.43	1.07	1.71	1.00	0.44	0.00	5.00

645